Electronic Supplementary Material (ESI) for Environmental Science: Nano.

Supporting Information

Development and Experimental Evaluation of a Mathematical Model to Predict Polymer-Enhanced Nanoparticle Mobility in Heterogeneous Formations

Hamed Mohammadnejad [a], *Bonnie A. Marion* [a], *Anthony A. Kmetz* [b], *Keith P. Johnson* [c]

Kurt D. Pennell [d], *Linda M. Abriola* [*a]

[a] Department of Civil and Environmental Engineering, Tufts University, Medford, Massachusetts 02155, United States

[b] Shell Techworks., Cambridge, Massachusetts, 02139, United States

[c] McKetta Department of Chemical Engineering, The University of Texas at Austin, Austin, Texas 78712, United States

[d] School of Engineering, Brown University, Providence, Rhode Island, 02912, United States

A. Nanoparticle retention results

Figure S1a is a photo of the flow cell at the end of the magnetic iron oxide nanoparticle (nMag) and Gum Arabic (GA) solution injection experiment. Here the region associated with particle retention can be delineated as that having a light brown color in the lower half of the cell. Numerical simulations of nMag retention (Figure S1b) suggests that substantially more nMag was retained in the lowest permeability lenses (CSS) than in the Ottawa sand lenses, predicting a sorbed mass concentration ranging between 100-830 μg nMag/g solid. Figure S2a shows the labeled zones inside the Markov box for nMag mass retention measurement where zones marked as G1, G2, G4, I1, I2 and I3 correspond to CSS lenses. Measured and simulated retained nMag in CSS lenses of the domain, along with the relative error ($error = 100 \times \frac{|measured - simulated|}{|measured|}$)are provided in Figure S2b. No retention values are reported herein for the Ottawa sands. For these materials, the confidence intervals for the iron measurements were too large to provide meaningful comparisons with simulated results. This is likely due to slight mixing of the CSS and the Ottawa sand media during packing, which would have a large impact on attachment, due to the 10-fold greater maximum sorption capacity (S_{max}) of CSS compared to Ottawa sand (see Table 2 in main text).

Simulated and measured values of retained mass in G1, G2, G4 and I1 are in reasonable agreement, with average relative errors below 20 percent. However, measured nMag retention in the I2 and I3 zones are significantly higher than the simulated values. The I2 and I3 zones are located deeper in the lens and the simulated nMag plume did not penetrate as far into those areas, in comparison to the experiment. It may be that the CSS lenses in this area of the box

had higher effective permeabilities, due to variable packing and/or mixing with other sand types, especially around the boundaries of lenses. Such heterogeneities in packing could not be quantified and were not accounted for in the simulation.

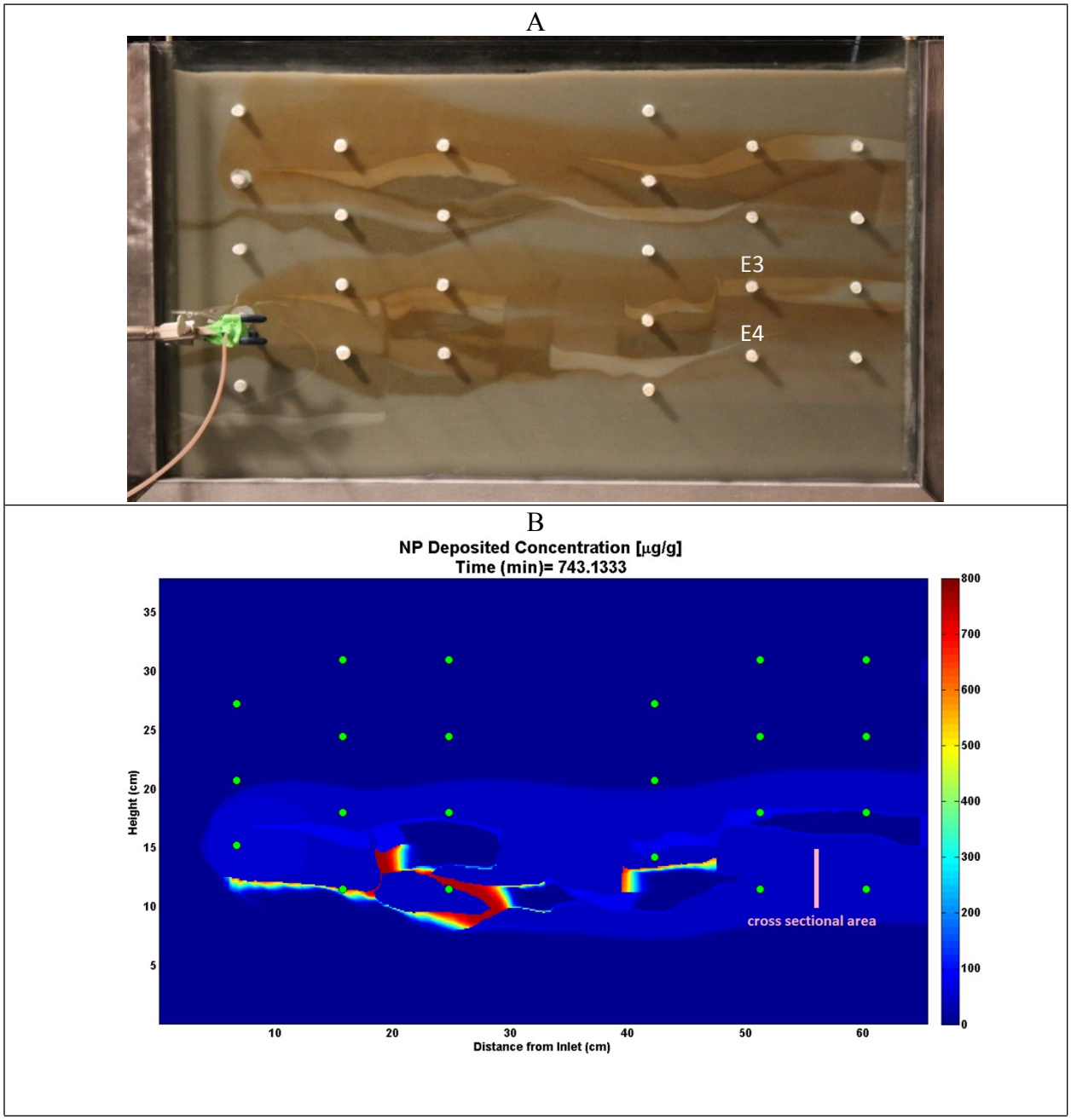

Figure S1. A) Sorbed mass profile of the nMag+GA injection at the end of the experiment. B) simulated retained mass in the sand in µg of nMag per gram of sand, pink colored cross sectional area (location: 56.75cm from the inlet and 10-15cm from the bottom) was employed in the attachment parameter uncertainty analysis.

(a)

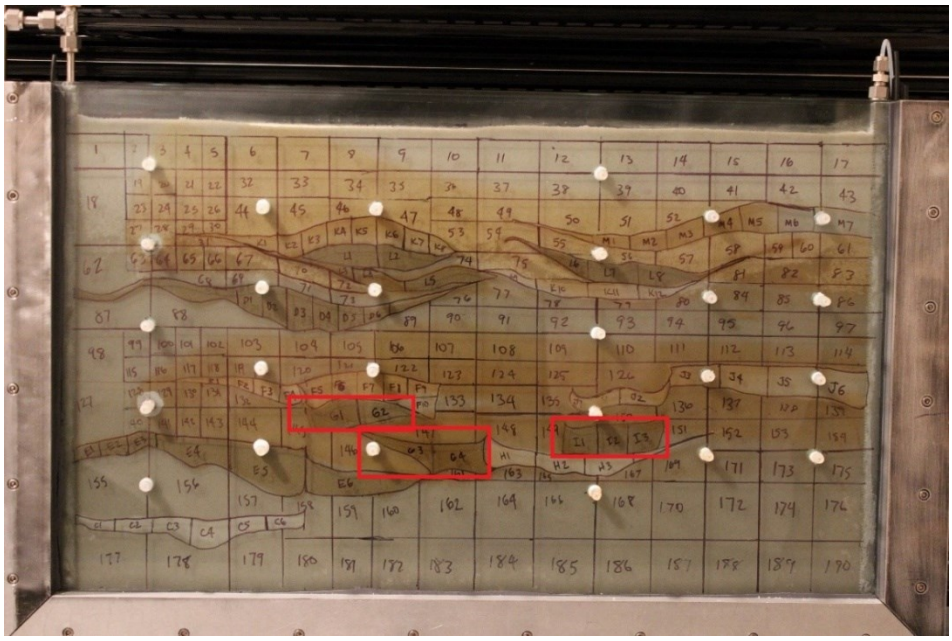

(b)

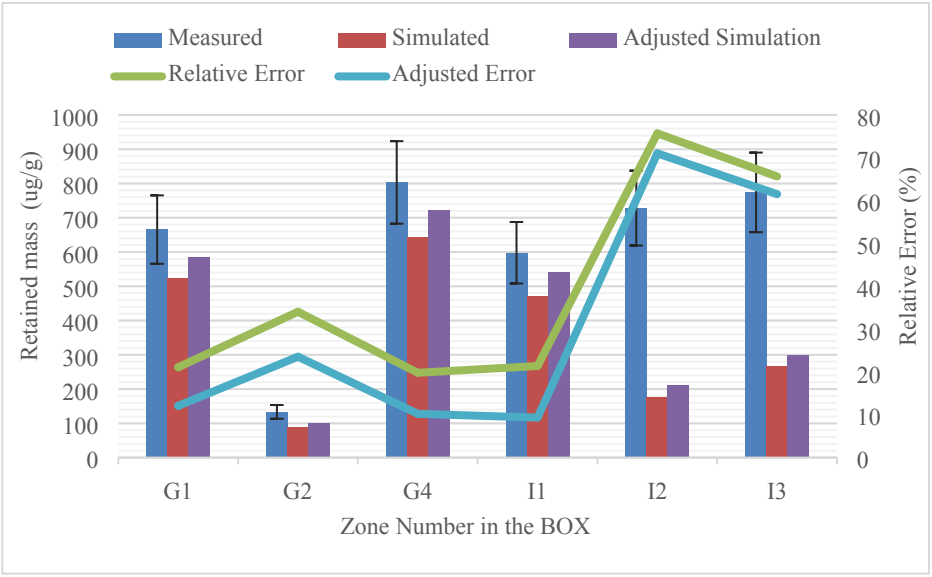

Figure S2) (a) Zone numbers inside Markov box for retention measurement (G1, G2, G4, I1, I2, I3) correspond to CSS lenses marked by red rectangles. (b) Measured, simulated, and adjusted simulation values of retained mass in the zone numbers are plotted in Figure S2a. The adjusted simulation and associated prediction errors correspond to the velocity-dependent attachment parameter sensitivity simulations conducted as described below. Plotted estimated error bars (denoting a 14.3% relative measurement standard deviation) are based upon a triplicate measurement of mass retention in I1.

B. Uncertainty analysis of nMag attachment parameters due to variations in pore velocity

According to previous NP transport studies[1], pore-water velocity can have a major impact on transport behavior of NPs, and thus, NP attachment parameters, k_{att} and $S_{max.NP}$, are expected to vary with pore-water velocity. Here, the impact of the uncertainty of the attachment parameters (due to variations in the pore-water velocity) on the flow cell simulation results is investigated through a limited sensitivity analysis.

Based on classical filtration theory (CFT) the first order attachment rate can be represented as:

$$k_{att} = \frac{3(1-\theta)v_p}{2d_c}\alpha\eta_0 \quad (1S)$$

$$\eta_0 = 2.4A_S^{0.33}N_R^{-0.081}N_{Pe}^{-0.715}N_{vdW}^{0.052} + 0.55A_s \quad (2S)$$

where d_c is a representative collector (i.e., grain) size (L) and α(-) is the attachment efficiency. Theoretical collector efficiency is represented by η_0(-) and can be estimated with a correlation presented by Tufenkji and Elimelech (eqn 2S)[2]; where A_s is the Happel correction factor, N_R is the interception number, N_{Pe} is the Peclet number, N_{vdW} is the London-van der Waals attractive forces number, N_A is the attraction number, and N_G is the gravitational number. η_0 is a function of velocity through its dependence on Peclet number. There were insufficient data in this study to fully quantify the dependence of k_{att} on pore-water velocity; however, the probable range of these parameters with variations in pore-water velocity can be estimated. As discussed in the results section of the manuscript, the average simulated pore-water velocities in 40-50 OS, 80-100 OS

and CSS were 2.04, 0.47 and 0.26 m/d, respectively, while fitted parameters were based on core flood experiments conducted at a pore velocity of 2 m/d. cell. Based on eqns (1S) and (2S) and the average and minimum pore water velocities, a range of k_{att} values was estimated for the sands (values provided in Table 1S). In order to estimate attachment efficiency α, fitted k_{att} from baseline cases along with estimated η_0 from eqn (2S) were used in eqn (1S). The computed attachment efficiency values were then assumed constant for a particular medium and used to estimate new attachment rates for pore velocities that differed from the baseline cases. Note that the average pore-water velocities within the 40-50 OS medium in the flow cell were close to the value used in the column experiments and k_{att} was not varied for this medium.

The value of $S_{max.NP}$ has also been shown to vary with pore-water velocity[3], attributed to a 'shadow zone effect', where a reduction in pore-water velocity will increase accessible NP attachment surface area. According to one previous column study of nMag mobility,[4] a 84 percent decrease in pore-water velocity resulted in a 15 percent increase in $S_{max.NP}$ for 80-100 OS. In Case 12 in Table 2 of this study a 3% increase in the value of $S_{max.NP}$ for CSS was observed when the column pore-water velocity was reduced from 10 to 2 m/d. Based on these data and the mean and minimum velocity values presented in Table 2S, $S_{max.NP}$ was increased for 80-100 OS by 15 to 30 percent of its column-fitted (baseline) value, and for CSS, $S_{max.NP}$ was varied by 20 to 40 percent of its baseline value (Table 1S).

Table 1S. Flow rate uncertainty analysis on nanoparticle attachment parameters and the impact on mass recovery.							
Case	Description	*Katt* [2] (1/hr)	v_p (m/d)	η_0 [3]	α [4]	$S_{max,NP}$ ($\mu g/g$)	Impact on mass recovery compared to baseline
1	80-100 OS Baseline [1]	2.51	1.95	0.17	0.03	108	-
2	80-100 OS lower k_{att}	1.60	0.47	0.45	0.03	108	<1%
3	80-100 OS lowest k_{att}	0.86	0.15	0.76	0.03	108	<1%
4	80-100 OS Higher $S_{max,NP}$	2.51	-	-	-	124	<-1%
5	80-100 OS Highest $S_{max,NP}$	2.51	-	-	-	140	-2%
6	CSS baseline [1]	4.2	2	0.25	0.016	1008	-
7	CSS lower k_{att}	2.2	0.26	1	0.016	1008	+5%
8	CSS lowest k_{att}	0.43	0.05	1	0.016	1008	+26%
9	CSS higher $S_{max,NP}$	4.2	-	-	-	1208	-7%
10	CSS highest $S_{max,NP}$	4.2	-	-	-	1409	-12%

[1] Baseline values for 80-100 OS and CSS were presented in case 4 and case 7 in Table 2 of the manuscript, respectively. [2] Lower and lowest k_{att} are based on average and minimum pore velocity within the lens, respectively and obtained from eqn (1S) using the attachment efficiency estimated for the baseline. [3] Collector efficiency was calculated from eqn (2S). [4] Attachment efficiency for the baseline was calculated from eqn (1S), based upon the fitted experimental attachment rate and calculated collector efficiency and kept unchanged for other velocities within the same medium.

The average concentration at the transect shown in Figure S1b was selected to illustrate the sensitivity of nMag mobility to uncertainties in attachment parameters ($S_{max.NP}$ and $k_{att,}$ Table 1S) in the lower permeability lenses. Here, the red curves in Figure S3a through S2d represent BTCs produced with fitted values of k_{att} and $S_{max.NP}$ obtained from column studies (Table S1 and Table 2). Dashed blue and blue lines show the results of the simulations employing variations of k_{att} and $S_{max.NP}$ over the selected ranges discussed above. Other parameters were kept constant, equal to the values presented in Table 2 in the manuscript.

Inspection of Figure S3 reveals that the CSS k_{att} value has a significant influence on the shape of the nMag concentration profile; a 50-90% reduction in k_{att} causes as much as 26% greater mass recovery (Case 7-8, Table 1S). Uncertainty of the maximum retention capacity value, $S_{max.NP}$, for CSS does not have as much impact as k_{att}, and the mass recovery reduction across the cross-sectional area was less than 12% (Case 9-10, Table 1S). Figures S3c and S3d show that uncertainty in 80-100 OS NP attachment parameters did not have a measurable influence on the NP transport in the box (cases 2-5 in Table S1), which can be attributed to the small volume of 80-100 OS in the box compared to the background media. Based upon the above analysis, attachment parameters for CSS were adjusted in the model, employing k_{att}=2.22/hr, $S_{max,NP}$=1208 μg/g, in place of the baseline values presented in case 7 of Table 2 in the manuscript. Application of these adjusted parameters led to a reduction in retained mass relative error by approximately 50% (Figure S2b).

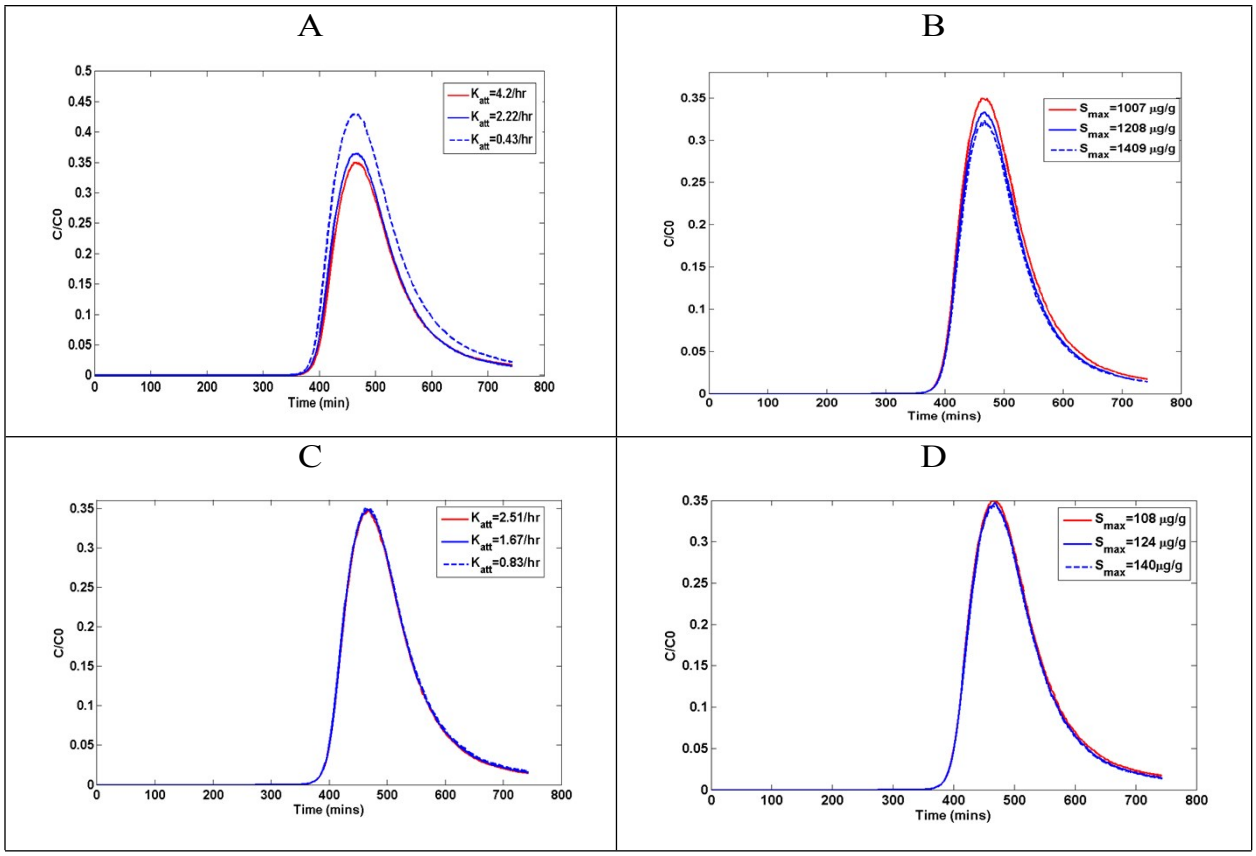

Figure S3. Sensitivity analysis of nMag breakthrough concentration at the cross sectional area to changes in (A) K_{att} in CSS (B) S_{max} in CC (C) K_{att} in 80-100 OS (D) S_{max} in 80-100 OS

References

1. I. Toloni, F. Lehmann and P. Ackerer, Modeling the effects of water velocity on TiO2 nanoparticles transport in saturated porous media, *Journal of contaminant hydrology*, 2014, **171**, 42-48.
2. N. Tufenkji and M. Elimelech, Correlation equation for predicting single-collector efficiency in physicochemical filtration in saturated porous media, *Environmental science & technology*, 2004, **38**, 529-536.
3. A. Taghavy and L. M. Abriola, Modeling reactive transport of polydisperse nanoparticles: assessment of the representative particle approach, *Environmental Science: Nano*, 2018, **5**, 2293-2303.
4. B. A. Lyon-Marion, M. D. Becker, A. A. Kmetz, E. Foster, K. P. Johnston, L. M. Abriola and K. D. Pennell, Simulation of magnetite nanoparticle mobility in a heterogeneous flow cell, *Environmental Science: Nano*, 2017, **4**, 1512-1524.